Array design considerations for exploitation of stable weakly dispersive modal pulses in the deep ocean

Ilya A. Udovydchenkov[a]

[a] *Communication, Navigation and Sensor Signal Processing Department, Electronic Systems and Technologies Technical Center, The MITRE Corporation, Bedford, MA, 01730, USA*
and
Geology and Geophysics Department, Woods Hole Oceanographic Institution, Woods Hole MA, 02543, USA

Abstract

Modal pulses are broadband contributions to an acoustic wave field with fixed mode number. Stable weakly dispersive modal pulses (SWDMPs) are special modal pulses that are characterized by weak dispersion and weak scattering-induced broadening and are thus suitable for communications applications. This paper investigates, using numerical simulations, receiver array requirements for recovering information carried by SWDMPs under various signal-to-noise ratio conditions without performing channel equalization. Two groups of weakly dispersive modal pulses are common in typical mid-latitude deep ocean environments: the lowest order modes (typically modes 1-3 at 75 Hz), and intermediate order modes whose waveguide invariant is near-zero (often around mode 20 at 75 Hz). Information loss is quantified by the bit error rate (BER) of a recovered binary phase-coded signal. With fixed receiver depths, low BERs (less than 1%) are achieved at ranges up to 400 km with three hydrophones for mode 1 with 90% probability and with 34 hydrophones for mode 20 with 80% probability. With optimal receiver depths, depending on propagation range, only a few, sometimes only two, hydrophones are often sufficient for low BERs, even with intermediate mode numbers. Full modal resolution is unnecessary to achieve low BERs. Thus, a flexible receiver array of autonomous vehicles can outperform a cabled array.

Keywords:
Ocean acoustics, weakly dispersive modal pulses, long-range sound propagation, underwater communications

Email address: ilya@whoi.edu (Ilya A. Udovydchenkov)

1. Introduction

A broadband acoustic wave field can be represented as a superposition of modal pulses [1, 2], which are broadband contributions to the wave field corresponding to fixed mode numbers. Stable weakly dispersive modal pulses (SWDMPs) are special modal pulses that are characterized by negligible dispersion and weak scattering-induced broadening. To appreciate the difference between SWDMPs and typical modal pulses, assume that the wave field is excited by a point source whose time history consists of two cycles of a carrier frequency. In that wave field the information carried by a SWDMP is a delayed replica of the transmitted signal, two cycles of the carrier frequency. In contrast, in the same wave field dispersion causes most other (typical) modal pulses to unravel into frequency-modulated sweeps whose duration grows with increasing range. The anomalous absence of unraveling of the SWDMPs leads to potentially important underwater acoustic communications applications. The received SWDMP waveform is to a good approximation a replica of the transmitted signal, thereby eliminating (under ideal circumstances) the need to equalize. The difference in behavior between SWDMPs and typical modal pulses can be explained by the fact that SWDMPs have the special property that the waveguide invariant for that mode number, evaluated at (or very near) the center frequency, is equal to zero. The extraction of a modal pulse, weakly dispersive or not, requires mode filtering. This paper investigates, using theoretical arguments and numerical simulations, the receiver array design requirements necessary to extract, from an acoustic wave field, an accurate estimate of a SWDMP, and, in turn, the information carried by it.

Simulations are performed in a nearly stratified ocean environment using a typical mid-latitude sound speed profile, in which two groups of weakly dispersive modal pulses commonly occur. The first group is the lowest order modes (modes 1-3 at 75 Hz are considered in the paper). The second group consists of intermediate order modes (around mode 20 at 75 Hz) whose waveguide invariant is near-zero. Broadband acoustic wave fields are simulated at ten equally spaced ranges between 50 km and 500 km with a point source transmitting a phase-modulated binary sequence. The resulting wave fields are mode processed using various receiver array configurations. The modal pulses are demodulated to estimate the transmitted binary sequence.

Signal distortions lead to inter-symbol interference (ISI) and are quantified by the bit error rate (BER) (the percentage of incorrectly detected bits), which is a convenient measure of the performance. No a priori receiver training or channel equalization is performed. To estimate uncertainties due to environmental variations, which in turn cause variations in the modal shapes, all simulations and post-processing steps are repeated 10 times with different realizations of the sound speed perturbation field.

One question that motivated this analysis is: Under what conditions can the information carried by a SWDMP be recovered with small errors (as measured by BERs) if the corresponding modes are not fully resolved? In the environments considered in this paper, which closely resemble a typical mid-latitude deep ocean sound speed profile, approximately 40 hydrophones are needed to resolve the first 10 modes at 75 Hz [3–6]. It turns out that low BERs can often be realized when the modes comprising a SWDMP are not fully resolved. It is shown that, for the lowest order modes, a surprisingly small number of hydrophones at fixed depths, sometimes as few as three, is needed to achieve low BERs at ranges up to 400 km. For the SWDMPs corresponding to modes 19 and 20 as few as 34 hydrophones at fixed depths may be needed to achieve low BERs. It is also shown that only two or four hydrophones may be sufficient to achieve low BERs for SWDMPs for low and intermediate mode numbers, respectively, if the receiver depths are optimally chosen depending on the horizontal distance to the source. Of course, one cannot expect an adequate resolution of any modes with only two hydrophones, or mode 20 at 75 Hz with only four hydrophones, but full modal resolution turns out to be unnecessary to achieve low BERs. With this analysis a portable and flexible receiver array composed of autonomous underwater vehicles (AUVs) will, in some instances, have superior communications performance to cabled arrays.

Since SWDMPs experience little propagation-induced distortion, they are useful in communications applications [7, 8]. The underwater acoustic channel is a challenging communications media due to the constantly fluctuating ocean environment and due to multipath propagation which results in large channel delay spread [9]. In a deep ocean long-range acoustic communication system, a signal consisting of a sequence of symbols experiences significant ISI (up to several seconds or hundreds of transmitted symbols [10]), which precludes achieving reliable high-speed data transmissions. A common solution is to design a receiver that compensates for the ISI and employs a decision feedback equalizer (DFE) [9]. However, large channel delay spread increases the complexity of the required DFE [11].

An important milestone in long-range underwater acoustic communications is the work of Freitag and Stojanovic [12]. The authors processed the acoustic data transmitted over 3250 km range using an adaptive multichannel DFE with integrated phase tracking and Doppler compensation and showed that the joint use of 20 hydrophones allowed near symbol-rate communications (37.5 bps). At this long range the channel spread is on the order of several seconds requiring many equalizer taps, but the computational complexity is partially mitigated by the low symbol-rate.

It is demonstrated in this paper that the extraction of information carried by SWDMPs prior to equalization reduces the channel delay spread by exploiting the physics of the underwater sound channel and the properties of the acoustic wave field, thus reducing the complexity of the DFE. Note that mode processing differs from reduced complexity equalization. The latter is designed to invert the distortions due to propagation through the channel. The mode-processed wave field, however, is still a solution to the acoustic wave equation. One possible extension of this analysis, which is outside of the current scope, is to revisit the receiving array requirements if modal analysis is combined with the equalization method presented in [12]. A disadvantage to our approach is that SWDMPs might not exist in a given environment for the ranges considered. While SWDMPs exist in many ocean environments, they are not ubiquitous.

SWDMPs are related to weakly divergent beams [7]. Weakly divergent beams were described theoretically in [13] and later in [14, 15] and they have been observed experimentally in the North Atlantic at ranges up to 3500 km [16–18] and in the Norwegian Sea at ranges up to 1000 km [19]. The connection between weakly divergent beams and SWDMPs arises from ray-mode duality: the asymptotic equivalence of acoustic wave fields described using rays or as a superposition of normal modes [20, 21]. Here we demonstrate that information carried by SWDMPs, even corresponding to intermediate mode numbers, can be recovered with a few hydrophones with their positions well-predicted by the asymptotic ray-mode duality results.

The remainder of the paper is organized as follows. Section II provides an example demonstrating that only two hydrophones could be sufficient to extract the information carried by a SWDMP corresponding to an intermediate order mode at 400 km range. Section III describes numerical simulations of acoustic wave fields and the processing algorithm used to estimate BERs. Section IV is divided into three subsections and presents the results relating to low order modes, to intermediate order modes, and to processing with minimal arrays. Minimal arrays have the fewest number of elements to achieve a given BER threshold, and the hydrophone depths are allowed to vary depending on the source-receiver distance. It is shown that full modal resolution is unnecessary to achieve low BERs. It is demonstrated that the optimal hydrophone depths can be well predicted using mode rays (rays whose action variable is determined by the quantization condition [2]) corresponding to the SWDMPs. The dependence of array requirements on signal-to-noise ratio (SNR) is also analyzed. Discussion of the results is presented in Section V. Conclusions are given in Section VI.

2. Motivating example: Why are SWDMPs special?

Two slightly different range-independent ocean sound speed profiles are considered in this paper. These profiles are shown in Figure 1. The first profile, called C0, is the canonical "Munk" mid-latitude ocean profile [22]. The second profile, C1, is the same as C0 with a Gaussian disturbance added in the upper ocean [23]. C1 qualitatively resembles an environment constructed from the hydrographic data in the Eastern North Pacific ocean [24]. The C0 profile can be thought of as a generic mid-latitude deep ocean sound speed profile for which low order modes are expected to be weakly dispersive. The C1 profile supports SWDMPs corresponding to intermediate order modes. This expectation is illustrated in the right panel of Figure 1, which shows the dependence of the waveguide invariant β [25, 26] on mode number at 75 Hz for both profiles. The theory of modal group time spreads [2, 6, 26, 27] predicts that the modal dispersion is largely controlled by the product $I(m, f)\beta(m, f)$, where I is the ray action, f is acoustic frequency, and m is the mode number. It follows from the asymptotic quantization condition (see, for example, Eq. (3) in [6]) that the ray action grows linearly with the mode number. Thus, in the C0 profile only modes with small I-values (low order modes) are weakly dispersive. However, the C1 profile also supports an intermediate range of mode numbers around $m = 20$ with near-zero β, which are also expected to be weakly dispersive.

It turns out that low BERs can often be achieved in a binary transmission with a non-mode-resolving receiving array without channel equalization, if one focuses on SWDMPs. To illustrate this observation consider the example shown in Figure 2 (the choice of simulation parameters is explained in Appendix A). Assume a typical stratified mid-latitude deep ocean environment

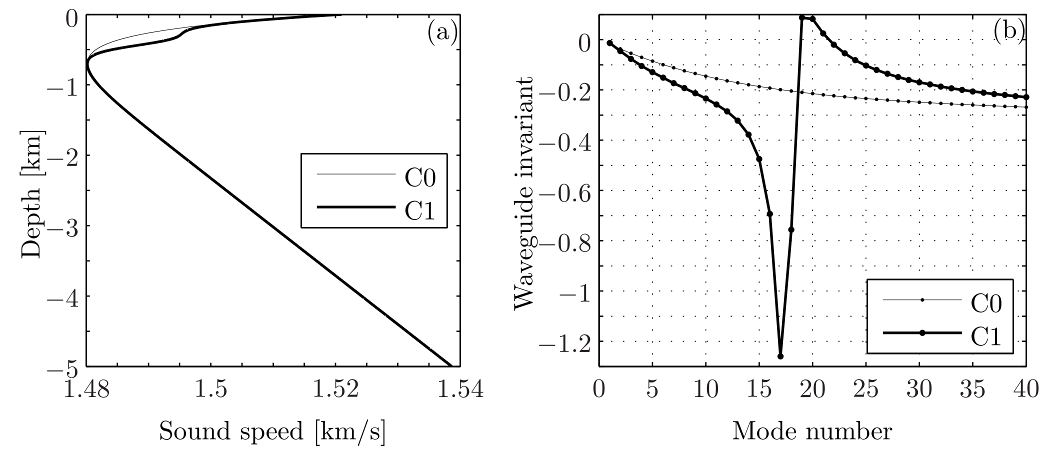

Figure 1: a) Two background sound-speed profiles considered in this paper: C0 is the canonical "Munk" profile and C1 is the same as C0 with a Gaussian disturbance added in the upper ocean. b) Waveguide invariant β at 75 Hz versus mode number in C0 and in C1.

with the background sound speed profile C1 shown in the left panel of Figure 1, on which a range- and depth-dependent sound speed perturbation due, for example, to internal waves (IWs) is superimposed. An acoustic source placed at 190 m depth transmits 1 binary digit which consists of 2 cycles of a phase-modulated signal with a 75 Hz carrier frequency. Figure 2a) shows the source function. Figures 2b) and 2c) show modal pulses corresponding to modes 20 and 30, respectively, at the source. Figure 2d) illustrates the mode 30 pulse arrival at 250 km range filtered using a dense receiving array. Significant pulse broadening and distortions are observed due to dispersion and scattering. Figure 2e) shows the mode 20 pulse at 250 km range filtered using the same dense receiving array. Unlike the mode 30 pulse, the shape of the mode 20 pulse is almost unchanged. The estimated shape of the mode 20 pulse obtained using only two hydrophones placed at 710 m and 740 m depths is shown in Figure 2f). While modal "cross-talk" is unavoidable in this example, the "cross-talk" does not prevent one from correctly estimating the modal arrival. In fact, in this example, BERs are zero in 7 out of 10 simulations with different realizations of the IW-induced sound speed perturbation field.

It is shown in Section IV that with the source transmitting a sequence of binary digits, even with SNR as low as 5 dB, the optimal placement of a

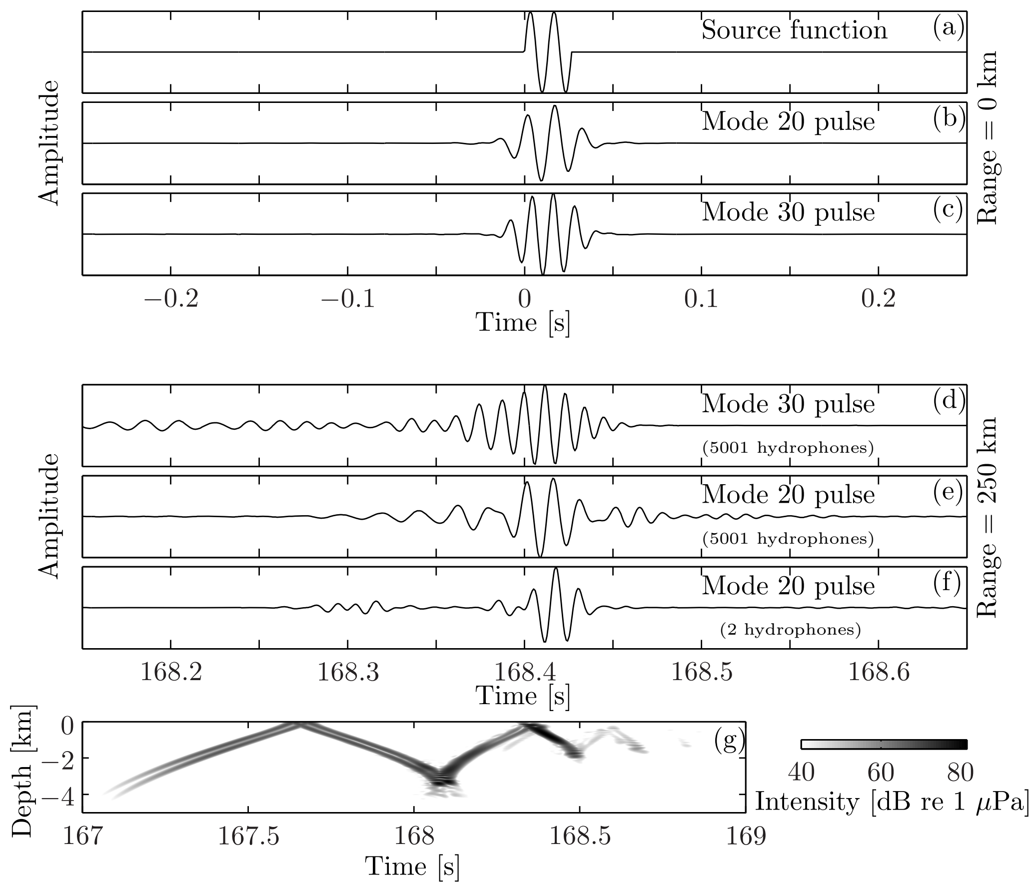

Figure 2: Evolution of the mode 20 and mode 30 pulses from the source to 250 km range. a) The source function showing one binary digit that consists of two cycles of the carrier frequency at 75 Hz. b) The mode 20 pulse at the source. c) The mode 30 pulse at the source. d) The mode 30 pulse at 250 km range filtered using 5001 hydrophones with 1 m spacing. e) The mode 20 pulse at 250 km range filtered using 5001 hydrophones with 1 m spacing. f) The mode 20 pulse at 250 km range processed using two hydrophones at 710 m and 740 m depth. All amplitudes are normalized to unity, except the mode 20 pulse amplitude at the source (b), which is normalized to the peak amplitude of the mode 30 pulse (c) to show that the mode 30 pulse is excited slightly stronger than the mode 20 pulse. g) The wave field intensity versus arrival time and depth at 250 km range produced by a point source placed at 190 m depth that transmits 1 binary digit.

few hydrophones often results in low BERs. In contrast, BERs are always high for the mode 30 pulse, even with high SNR and a dense receiving array covering the entire water column. So, how is it possible that BERs for some modal pulses are small or even zero with a non-mode-resolving array, while for other modal pulses even a dense mode-resolving array covering the entire water column results in high BERs? The large differences between Figures 2d) and 2e) (or 2d) and 2f)) arise because SWDMPs (the mode 20 pulse in this example) are special: they experience almost no distortion due to dispersion and scattering along the propagation path. Also, similarities between Figures 2e) and 2f) suggest that perfect modal resolution is unnecessary to correctly identify digits, and only a few hydrophones could be sufficient. This paper investigates the design of a communications system that takes the most advantage of the special properties of SWDMPs in the deep ocean.

It is important to note that the receiving array geometry and the source depth in this motivating example are chosen to efficiently excite the mode 20 pulse, which propagates in the C1 environment to long ranges with minimal distortion. The results of these considerations can also be illustrated by plotting the wave field intensity versus arrival time and depth as shown in Figure 2g), which is an approximation to the underwater channel impulse response (the impulse in this case is 1 binary digit consisting of 2 cycles of the carrier frequency). The energy corresponding to the mode 20 pulse appears as a contribution to the high intensity arrival with small time spread at around 168.42 s. Note, however, that if one does not focus on the minimally spread mode 20 pulse, the receiver has to compensate for the propagation-induced distortions in that high intensity arrival and for other distorted arrivals.

These studies are also motivated by results from the Long-range Ocean Acoustic Propagation EXperiment (LOAPEX) [28, 29]. It was shown, using these experimental data [8], that low order mode SWDMPs propagate in the Eastern North Pacific ocean without significant distortions up to 500 km range. In that experiment, a vertical line array of hydrophones with 40 elements was used. The array covered depths between approximately 350 m and 1750 m with 35 m spacing between hydrophones. Unfortunately, that array did not resolve mode numbers higher than approximately 10. Thus, it was not possible to utilize SWDMPs corresponding to intermediate mode numbers. Numerical simulations presented here address this issue and estimate the least number of hydrophones needed for low BERs with either low or intermediate order SWDMPs.

3. Numerical simulations. Acoustic propagation modeling and post-processing of simulated wave fields

Numerically simulated wave fields are constructed using the range-dependent acoustic propagation model RAM [30, 31]. The details are summarized in Appendix A. These wave fields have been compared with the wave fields computed using a split-step Fourier PE model [32] and excellent agreement was observed.

Figure 3 shows an example of the simulated acoustic wave field and the corresponding mode 1 arrival at 500 km range in the C0 profile with the IW-induced perturbation superimposed. The point source is placed at 800 m depth (the same depth that was used in LOAPEX). Figure 3a) shows the wave field intensity as a function of depth and time resulting from a 1023-digit m-sequence transmission. Figure 3b) shows the wave field in panel (a) after pulse compression. Figures 3c) and 3d) show the mode 1 arrival, obtained from the wave fields in the corresponding top panels, before pulse compression and after pulse compression, respectively. To quantify the dependence of BERs on SNR we consider the wave field before pulse compression, such as shown in Figure 3a) and simulate ambient noise as uniformly distributed in depth and in time with levels relative to the highest rms signal pressure level over depth. For computational feasibility, four levels of SNR are considered: 5, 10, 15, and 20 dB. The LOAPEX data analysis (not discussed in this paper) suggests that these element-level SNR values are realistic at propagation ranges up to 500 km, though a more powerful source might be needed to achieve the highest 20 dB SNR at 500 km range. While this noise model might be considered an oversimplification, it is adequate to demonstrate the usefulness of the SWDMPs. More complex data-driven noise models would be needed to accurately account for the spatial correlation properties of the noise field. The simulated wave fields are obtained at ten equally spaced ranges between 50 km and 500 km in both profiles, C0 and C1, with the IW-induced perturbations superimposed. To reduce computational complexity only 10 different realizations of the IW-induced perturbation fields are considered. Thus, the probability of achieving a certain BER with a given array geometry is estimated in 10% increments.

Now the post-processing steps of the simulated wave fields, such as shown in Figure 3a), are discussed. From the analysis of the LOAPEX data [8] modes 1-3 are expected to be weakly dispersive in a canonical profile, so we focus on these modes first.

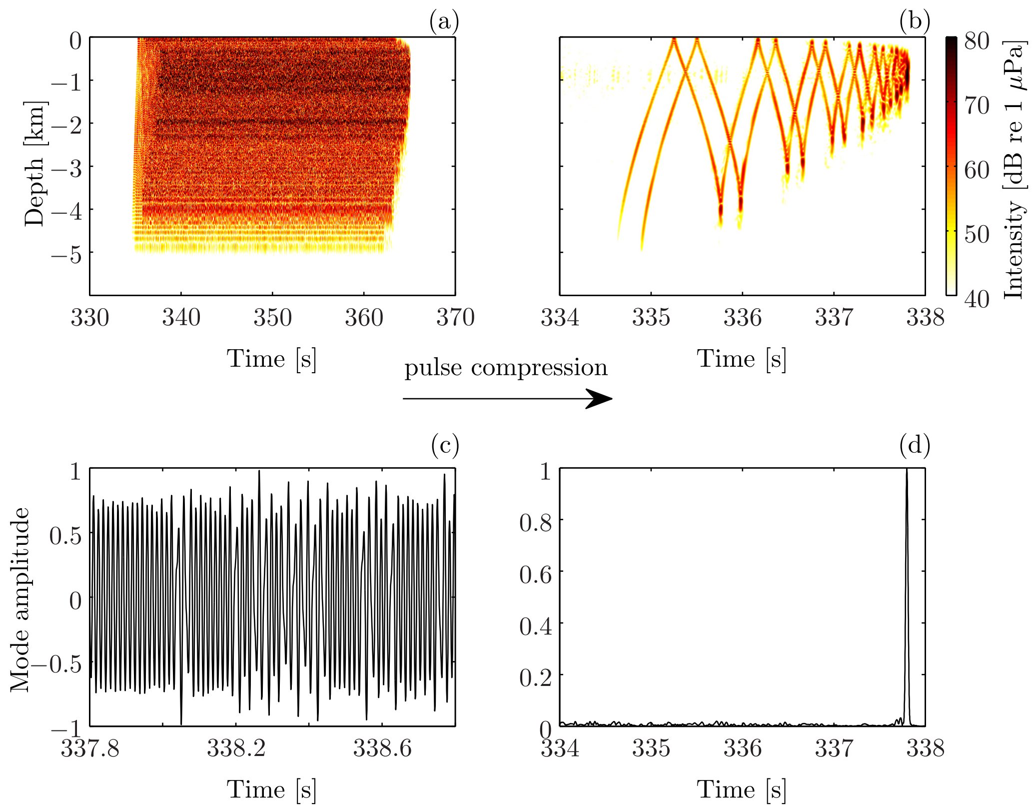

Figure 3: (Color online). The broadband acoustic wave field and the mode 1 arrival simulated at 500 km range in the C0 profile with the IW-induced perturbation superimposed. a) The wave field intensity versus arrival time and depth before pulse compression produced by a point source at 800 m depth with the 75 Hz carrier frequency emitting a phase-modulated m-sequence. b) The wave field in (a) after pulse compression (matched filtering). c) The mode 1 arrival of the mode-processed wave field shown in (a). d) The mode 1 arrival after pulse compression. Note that the mode 1 arrival in (d) may be obtained either by pulse compression of the mode 1 arrival in (c), or by mode filtering of the wave field in (b). The mode filtering was performed with a long and dense array sufficient to resolve all propagating modes.

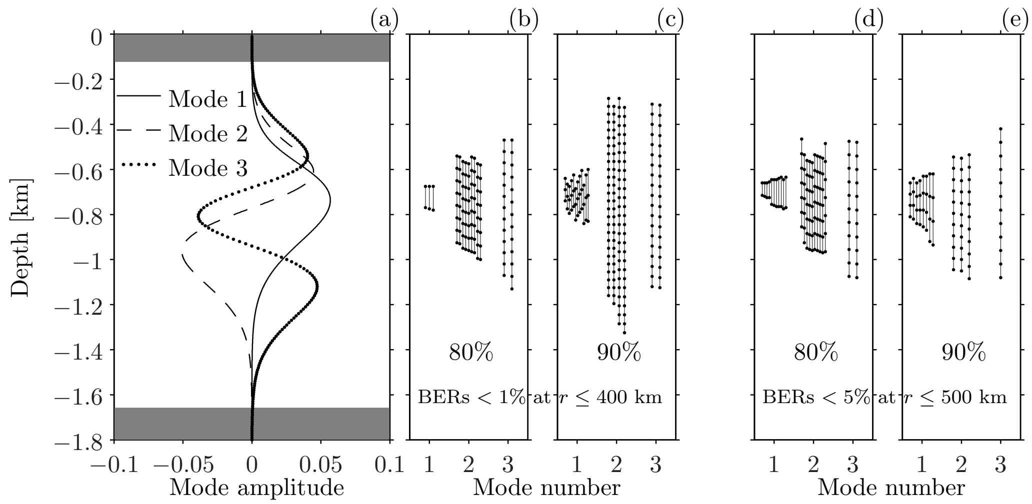

Figure 4: a) Modes 1, 2, and 3 computed at 37.5 Hz in the C0 profile. The domain of interest lies between 120 m and 1660 m (unshaded area). b) Array configurations resulting in BERs of less than 1% with 80% probability, at all eight ranges simultaneously up to 400 km, from processing of modes 1, 2, and 3 with a simulated SNR=20 dB. c) Array configurations resulting in BERs of less than 1% with 90% probability, at all eight ranges simultaneously up to 400 km, from processing of modes 1, 2, and 3 with a simulated SNR=20 dB. d) Same as panel (b), but with BERs of less than 5% at ten ranges up to 500 km. e) Same as panel (c), but with BERs of less than 5% at ten ranges up to 500 km. Note that the mode numbers are integers and the array configurations are offset horizontally from the integer marks for visualization purposes.

It is computationally prohibitive to test all possible receiving array configurations, so some simplifications are made. The lowest frequency of interest, 37.5 Hz, is chosen as the first null in the spectrum of the m-sequence modulated with two cycles of the 75 Hz carrier per digit (see Appendix A). The depth domain in which the mode 3 amplitude at this frequency is negligible (less than 40 dB below its peak value) is truncated as shown in Figure 4a) by gray shaded areas. The remaining test depths are between 120 m and 1660 m. Each tested array is uniquely defined by three parameters: the number of hydrophones, the separation between hydrophones, and the depth of the shallowest hydrophone. The minimum hydrophone separation is 5 m. The separation increment is also 5 m (only arrays with equal hydrophone separations of 5 m, 10 m, 15 m, etc. are tested). The depth-step for the shallowest hydrophones is also 5 m. The number of hydrophones in a test array varies between 2 and 309. For the low mode number analysis, a total of 257,292 arrays are tested. More details describing the selected array configurations are given in Appendix B.

To quantify the performance of these arrays the wave fields are mode processed and demodulated. The details of the demodulation are explained in Section III in [8]. To extract the binary sequence from carrier-modulated modal amplitudes $a_m(t)$ the following procedure was used. First, the signal was bandpass filtered between 50 and 100 Hz and then complex demodulated to baseband. Instantaneous phase $Y_m(t)$ and envelope signal $A_m(t)$ time series were computed for each transmission using a zero-phase forward-and-reverse 5-th order lowpass Butterworth filter [33, 34]. Discrete samples of the phase $Y_m(t)$ (sampled at 1200 Hz) were grouped into bins containing 32 samples (one digit is two cycles of the carrier; in the signal sampled at 16 times the carrier one digit contains 32 samples), and values within each bin were averaged. Because the transmitted sequence was a binary sequence, only the sign was retained after averaging. (For convenience we shall refer to the bits as $+$ and $-$ bits, corresponding to the sign of the phase modulation angle of the transmitted binary sequence.) Binary sequences derived from each transmission for each m-value were compared with the transmitted sequence bit-by-bit. The BER is the fraction (often expressed as a percentage) of the 1023 transmitted bits that are incorrectly identified. The zero-crossings of $Y_m(t)$ identify the times at which the phase polarity of successive incoming digits is reversed. The number of samples between any two zero-crossings should be a multiple of 32.

To implement this algorithm one needs to synchronize the incoming signal with the binary sequence. In other words, it is necessary to find the reference point in time at which a digit begins. Two considerations need to be taken into account. First, it is necessary to know how to group samples into bins of 32, i.e., to identify which of the 32 samples is the closest to the beginning of the digit. This can be accomplished by circular shifting the received signal by k samples, where k is an integer between 0 and 31. In practice one also needs to make sure that the synchronization time is not off by more than one digit, so in the actual implementation we varied k between -32 and 64. The second problem is to synchronize the initial phase, because the beginning of a digit, in general, does not coincide with a sampling point. This can be accomplished by shifting the phase of the signal by φ_0, which can vary between $-\pi$ and π. We did not attempt to find an efficient method to estimate k and φ_0 (which likely can be done from an analysis of incoming receptions). Instead, a brute force search that minimizes BERs of the signal recorded with a mode-resolving array was implemented to determine k and φ_0 for each $a_m(t)$.

Many of the array configurations tested are not mode resolving and do not allow accurate estimation of modal amplitudes and phases. Here discrete direct projection [4, 5, 35] is used no matter how sparse or short the test array is (even with only two elements). This processing results in modal "cross-talk". However, such analysis is still useful if one focuses on SWDMPs and one is only interested in finding phase transitions between the received digits. We refer to this analysis as "mode processing" as opposed to "mode filtering" (as shown in Figure 3), where the array is sufficiently long and dense to isolate individual modes. This mode processing can also be thought of as a computation of a weighted sum of received signals with modal eigenfunction values at the receiver depths.

4. Results

4.1. Low order modes

First, we focus on low order modes and the simulations performed in the C0 background profile with the IW-induced perturbation superimposed. Since the transmitted signal is known, one can compute BERs for all possible array configurations. Figures 4b) and 4c) show array configurations with the smallest number of hydrophones that resulted in BERs of less than 1% after processing modes 1-3 with all hydrophone depths fixed *at all eight ranges simultaneously up to 400 km.* Figure 4b) shows arrays that achieve BERs of less than 1% with 80% probability (in 8 out of 10 realizations). Figure 4c) shows arrays that achieve the desired BERs with 90% probability. Figures 4d) and 4e) are constructed similarly, except that the desired BER threshold is relaxed to 5% and the propagation range is extended to 500 km (the ranges of 450 km and 500 km were included). Only a subset of all configurations is shown for mode 1 in Figures 4c), 4d), and 4e).

These simulations show that two hydrophones are sufficient to achieve BERs of less than 1% with 80% probability by processing mode 1 at ranges up to 400 km. The number of required hydrophones is larger for modes 2 and 3 if BERs of less than 1% are desired. However, only 7-12 hydrophones are sufficient with mode 2 (or 3) processing at ranges up to 500 km to achieve BERs of less than 5% with 80% (or 90%) probability, provided the SNR is high (20 dB).

Several interesting conclusions can be made from Figure 4. First, a remarkably small number of hydrophones (2-4) are needed to achieve low BERs by processing mode 1 at ranges up to 500 km. This is a consequence of the simple mode 1 shape in depth. Second, Figure 4c) suggests that mode 2 processing could require more hydrophones than mode 3 to achieve low BERs. This is a consequence of the energy redistribution among modes due to scattering along the propagation path. At some intermediate ranges the amplitude of mode 2 (as computed with the fully mode-resolving array) is significantly lower than the amplitude of modes 1 or 3. In Figure 4c) the amplitude of mode 2 is low at some range in two or more realizations of the IW-induced perturbation field. Consequently, BERs of less than 1% with 90% success are difficult to achieve and a long array (35 hydrophones) is required to overcome low SNR. (Do not confuse this SNR, which is estimated from the mode amplitude, with the SNR used to simulate the acoustic wave fields, defined in Section III). Thus, the variations of modal energy along the propagation path are important. Third, the hydrophone spacing in arrays resulting in low BERs varies between 50 m and 135 m for mode 1, between 35 m and 80 m for mode 2, and between 45 m and 60 m for mode 3. In all cases the spacing is equal to a few wavelengths at 75 Hz, but is small enough to sample the mode shape structure. Finally, the array configuration corresponding to mode 3 shown in Figure 4e) does not span the depth aperture of mode 3. It is clear that the array is not mode resolving yet the weighted sum of contributions from mode 3 is sufficient to achieve low BERs.

One important objective of this work is to study the array requirements depending on SNR. Acoustic wave fields with different SNR levels are simu-

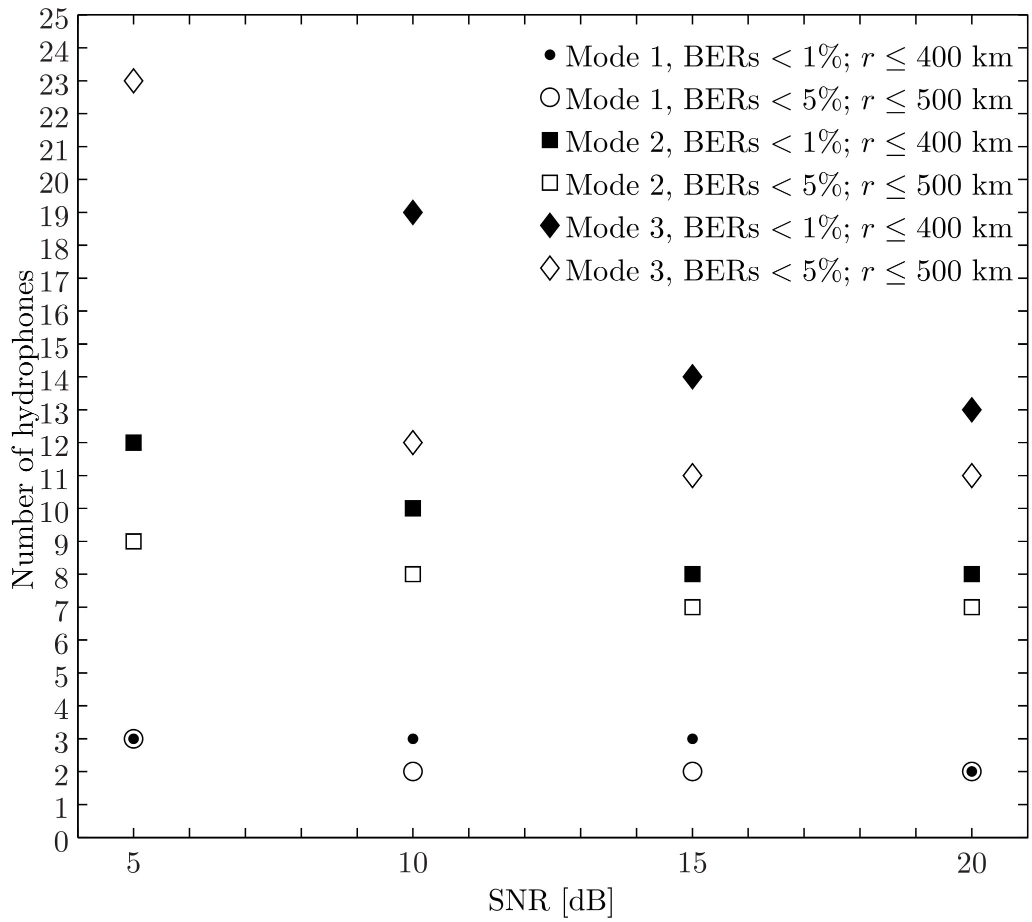

Figure 5: The number of hydrophones required to achieve either BERs of less than 1% at ranges up to 400 km or BERs of less than 5% at ranges up to 500 km with 80% probability by processing modes 1-3 for various SNRs. Sixty-three hydrophones are required to achieve BERs $< 1\%$ at $r \leq 400$ km by processing mode 3 with an SNR of 5 dB (not shown).

lated as explained in Section III. The least number of hydrophones required to achieve BERs of less than 1% at ranges up to 400 km or BERs of less than 5% at ranges up to 500 km with 80% probability for each SNR value is shown in Figure 5 for modes 1-3. At an SNR of 20 dB these results are consistent with Figures 4b) and 4d). With decreasing SNR, the number of required hydrophones increases, as expected. However, the mode processing results of mode 1 are so robust, that even with an SNR of 5 dB low BERs can be achieved with just three hydrophones at all ranges. As expected, mode 1 results are the most stable among the three modes because of the simplest structure of the mode 1 shape function in depth.

4.2. Intermediate order modes with a near-zero waveguide invariant

In this section the results obtained in the C1 background profile with IW-induced perturbations superimposed are summarized. The focus here is on intermediate mode numbers, for which the absolute value of the waveguide invariant is close to zero, and their utility as SWDMPs.

It is necessary to emphasize an important distinction between low order modes and intermediate order modes. To excite low order modes the source depth should be near the sound channel axis. Then all low order modes are excited, except those having a null at the source depth. This is suboptimal, however, for the excitation of intermediate order modes. First, one needs to choose which mode numbers to excite. The right panel of Figure 1 suggests that modes between approximately 19 and 23 might be weakly dispersive, because the corresponding values of the waveguide invariant β are close to 0. Strong excitation of mode 19 might not be desirable, however, because energy can scatter into adjacent modes (18, 17, etc.) along the propagation path, which are not weakly dispersive and have large negative values of β. The energy then scatters back into mode 19 and the modal pulse spreads in time. Since it is impossible to excite only one mode with a point source, it is better to "change" the source depth towards exciting higher order modes. A way to estimate an optimal source depth is shown in Figure 6. This figure shows the dependence of the waveguide invariant β on frequency for modes 19 and 20 constructed using the asymptotic quantization condition [26]. It is desirable to excite modes at those frequencies for which β is close to 0.

To estimate the source depth an arbitrary threshold of 0.15 is chosen and the frequency bands within which $|\beta| < 0.15$ are selected for mode numbers 19 and 20. The source depth of 190 m is computed as the mean value of the upper turning points (first nulls of the second derivative of the modal

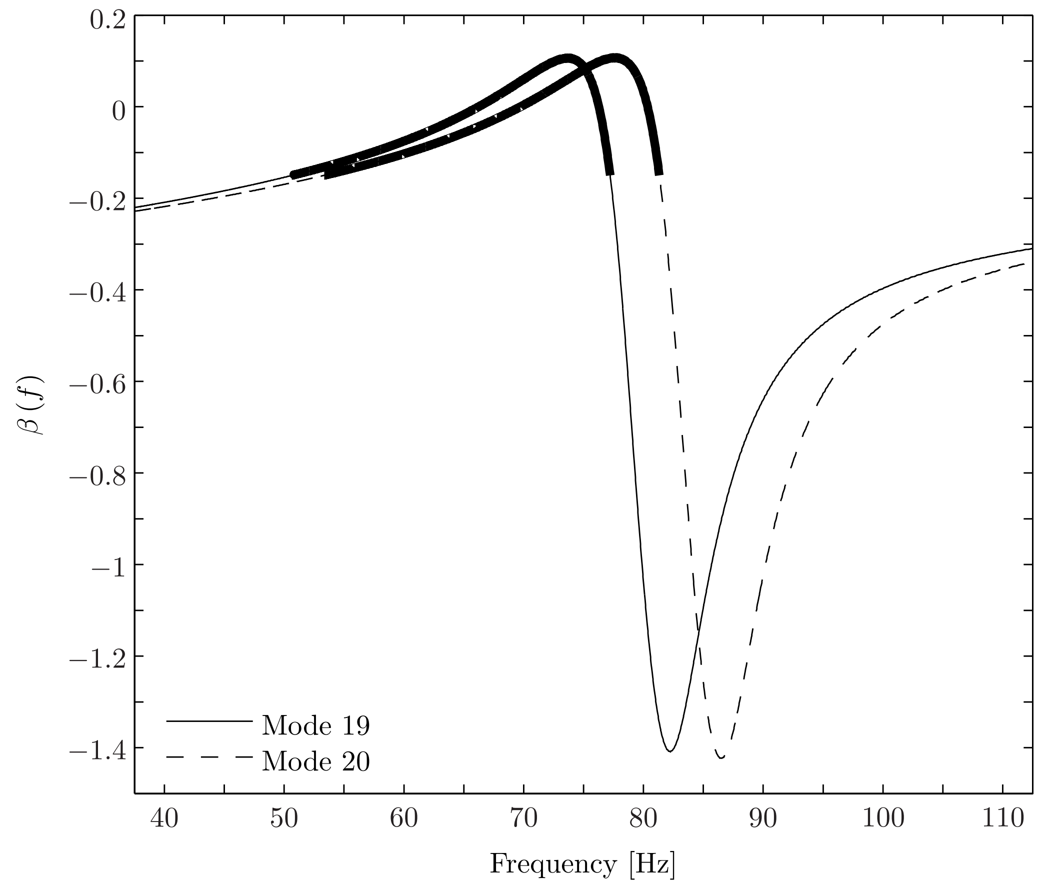

Figure 6: The waveguide invariant (β) dependence on frequency for modes 19 and 20. The frequency bands within which $|\beta| < 0.15$ are shown in bold. The source should be placed at a depth where it will excite modes at these frequencies. The estimated optimal source depth is 190 m.

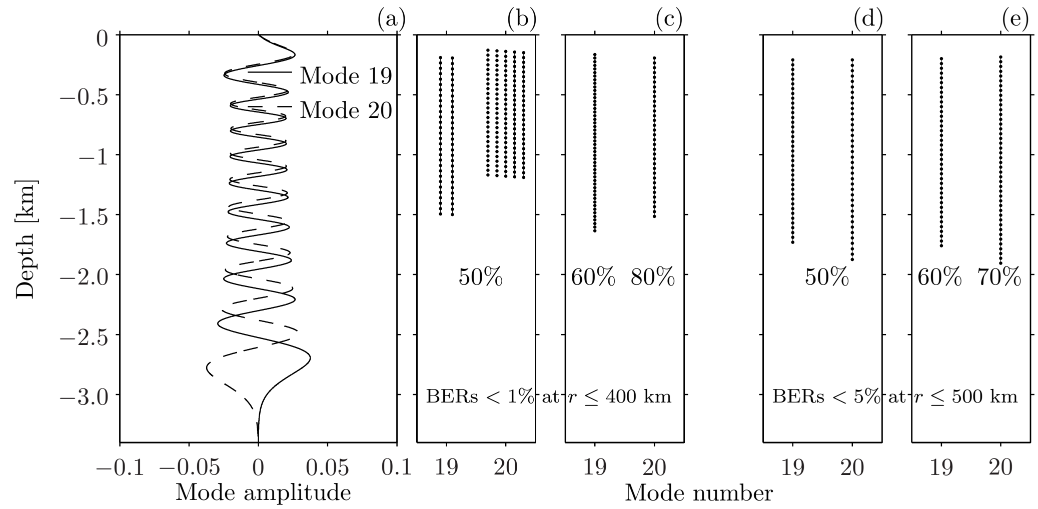

Figure 7: a) Modes 19 and 20 computed at 37.5 Hz in the C1 profile. The domain of interest is between the ocean surface and 3400 m depth. b-e) Arrays that resulted in BERs not exceeding a given threshold (1% or 5%) at ranges up to 400 km or 500 km with respective probabilities. These panels are constructed similarly to Figures 4b)-4e).

shape functions) of modes 19 and 20. Variations of the threshold imposed on $|\beta|$ showed little sensitivity in the source depth estimate. A set of full wave numerical simulations with a full water column array is performed with source depths around 190 m to confirm the lowest BERs for modes 19 and 20 at long ranges.

The analysis for modal pulses corresponding to modes 19 and 20 is similar to the analysis for low order modes. The spacing model between hydrophones is the same as for low order modes, but the maximum number of hydrophones in the tested arrays is increased to cover a depth aperture of 3400 m resulting in a total of 1,432,727 combinations.

Figure 7 is constructed similarly to Figure 4. However, the probabilities of achieving the desired BERs are lowered from 80% and 90% to the values between 50% and 80%. In all cases the arrays resulting in low BERs do not span the mode aperture of either mode 19 or 20. Despite the finer structure of modes 19 and 20 in depth, the separation between hydrophones that results in low BERs is between 30 m and 45 m, which is again a few wavelengths.

This analysis shows that low BERs are still achieved at ranges up to 400 km provided SNR is sufficiently high. Figure 8 shows the number of hydrophones required to achieve low BERs for modes 19 and 20 versus SNR.

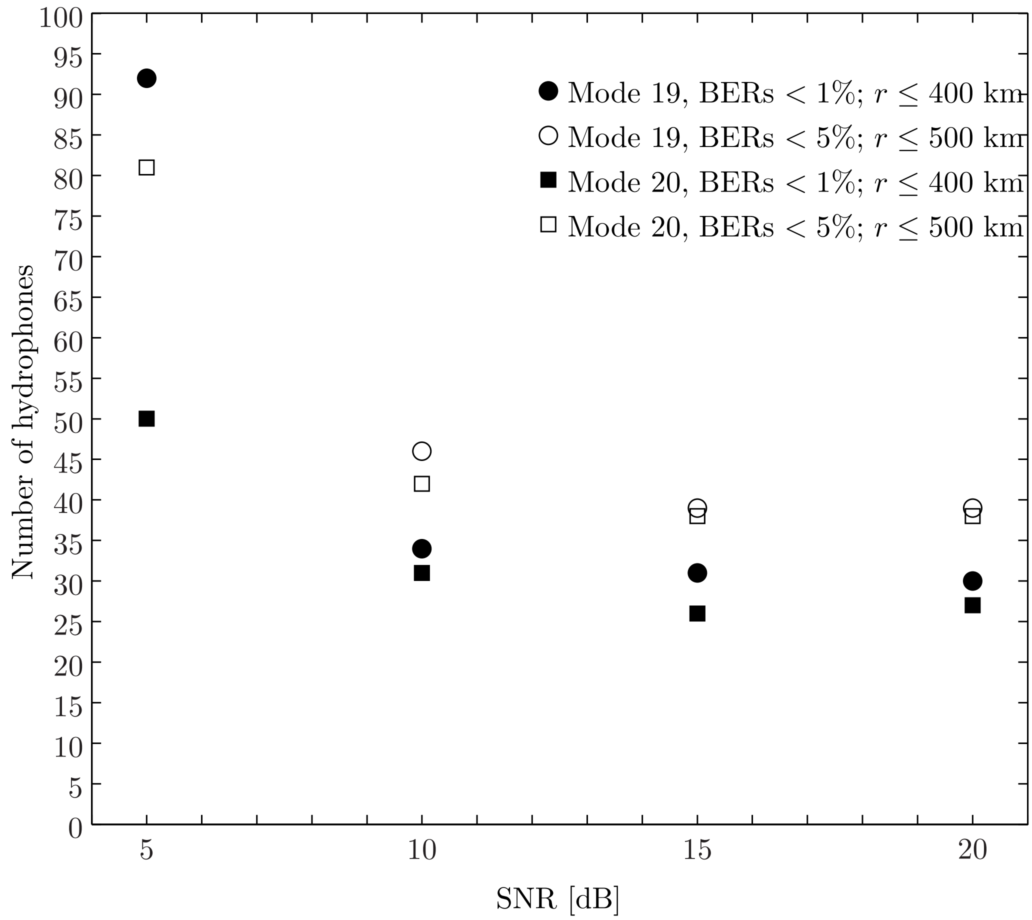

Figure 8: The number of hydrophones required to achieve either BERs of less than 1% at ranges up to 400 km or BERs of less than 5% at ranges up to 500 km with 50% probability using processing of modes 19 and 20 for various SNRs. One hundred and fifty-eight hydrophones are required to achieve BERs $< 5\%$ at $r \leq 500$ km by processing mode 19 with an SNR of 5 dB (not shown).

Table 1: The least number of hydrophones, at optimal receiver depths, required to achieve BERs of less than 1% at ranges up to 400 km as a function of mode number and SNR. Three values in each cell of the table correspond to the probabilities of 50%, 80%, and 90%. The infinity symbol means that no arrays satisfy the desired criteria.

C0

(a)

Mode number \ SNR [dB]	20	15	10	5
1	2,2,2	2,2,2	2,2,2	2,2,3
2	2,5,9	2,5,9	2,6,10	2,11,25
3	4,11,15	5,13,19	6,15,50	9,36,∞

C1

(b)

Mode number \ SNR [dB]	20	15	10	5
19	4,13,∞	4,13,∞	6,17,∞	9,58,∞
20	3,12,17	4,12,20	4,14,28	6,23,83

Approximately 30 hydrophones are needed for either mode 19 or 20, if the depths of the hydrophones are fixed for all eight source-receiver ranges up to 400 km. The required number of hydrophones increases rapidly with SNR falling below approximately 10 dB. Overall, these results are promising, as they demonstrate that the required number of hydrophones for achieving low BERs is smaller than one initially expects (several hydrophones per wavelength).

4.3. Mode processing with minimal arrays

Only a few hydrophones are often sufficient to achieve low BERs for either low or intermediate order modes, if the depths of the hydrophones on the test array are not restricted to be the same for all transmission ranges. The performance of such a system and its limitations are discussed in this section.

Table 1 shows the least number of hydrophones required to achieve BERs of less than 1% at ranges up to 400 km as a function of mode number and SNR. The three values in each cell of the table correspond to the probabilities of 50%, 80%, and 90%. Two hydrophones are sufficient with mode 1 processing for almost any SNR and desirable success rate. Generally, among the first 3 modes (Table 1a)), the number of required hydrophones increases with increasing mode number and decreasing SNR. The results re-emphasize the conclusion that energy redistribution among modes along the propagation path is important. This is why the number of required hydrophones rapidly increases at low SNRs for the 90% success rate.

Surprisingly, only a few hydrophones are required to achieve low BERs with SWDMPs corresponding to modes 19 and 20 (Table 1b)). Even with the lowest SNR of 5 dB, the number of required hydrophones is less than 10, provided the desirable success rate is not too high (50% in this case). Only 3 hydrophones are sufficient for a mode 20 pulse if the SNR is high. One should not be confused, however, regarding the "50% success rate" of the system. The success rate of 50% means that in half of the transmissions BERs at the receiver, decoding a 1023-digit sequence, are less than 1% (or 5% in some examples discussed above), and another half of the transmissions had errors greater than 1%. This, of course, *does not* mean that 50% of the transmitted information is decoded incorrectly. A practical advantage of this analysis is that systems with a few hydrophones are easier to deploy and operate, so the reduced success rate is a reasonable trade-off between performance and feasibility.

The dependence of BERs on the number of hydrophones in the receiving array is complex. Depending on environmental conditions and source and receiver depths one might achieve low BERs without equalization even with a single hydrophone. This typically occurs if the propagation range is sufficiently short. In this case, obviously, there is no benefit from modal analysis. As propagation range increases, it is beneficial to increase the number of receivers to estimate the desired SWDMP more accurately. It is difficult to predict, however, how much improvement, if any, would be achieved if a single hydrophone or a few hydrophones are added to an existing system.

As an example, consider an array consisting of 3 hydrophones at 590 m, 650 m, and 710 m depths in the C0 environment. Processing of mode 1 with this array at 500 km propagation range results in BERs of less than 1% in 9 out of 10 simulations (i.e. with 90% probability). With any subset of this array, the chance of achieving BERs of less than 1% does not exceed 60%. So, in this example an addition of the third hydrophone to the existing 2-hydrophone array increases the chance of reception at 500 km with less than 1% BER from 60% to 90%. Unfortunately, it is computationally intractable task to quantify in general the significance of adding an extra hydrophone to an existing array of an arbitrary length and configuration.

How does one find the depths of hydrophones that result in low BERs? While there is no simple rule that guarantees that desired positions can be found without prior measurements of the wave field, some guidelines can be offered. These guidelines are based on the results shown in Figure 9. In this figure two mode numbers are considered: mode 1 in the C0 profile, shown in Figure 9a), and mode 20 in the C1 profile, shown in Figure 9c). The SNR level was 10 dB. All two-hydrophone arrays that resulted in BERs of less

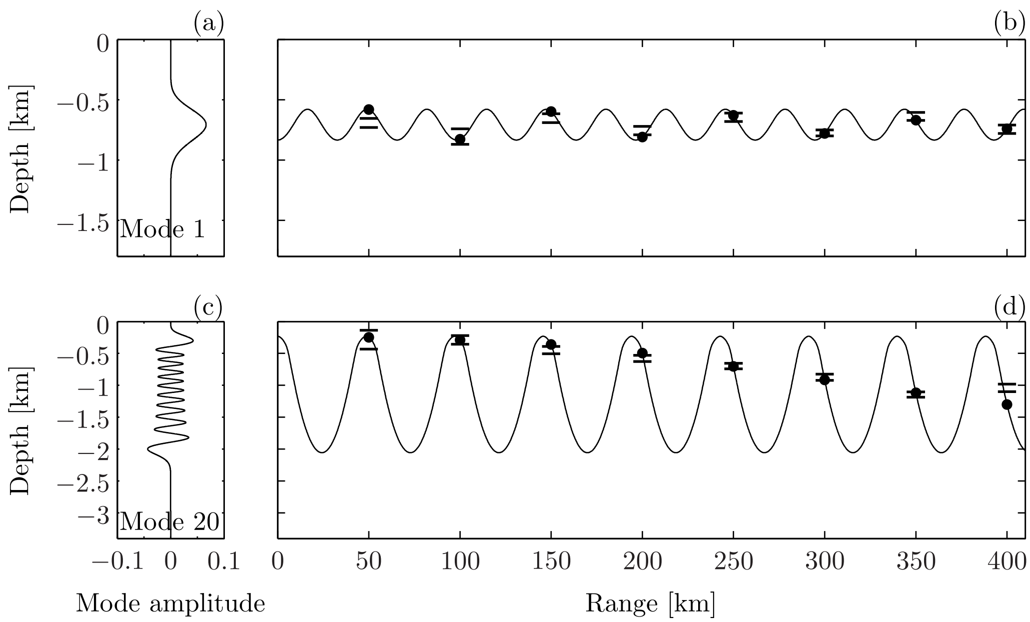

Figure 9: Estimating hydrophone depth for low BERs. a) Mode 1 in the C0 profile at 75 Hz. b) Depth estimates for two-hydrophone arrays that resulted in BERs of less than 1% with an SNR of 10 dB and a probability of 90%. c) Mode 20 in the C1 profile at 75 Hz. d) Depth estimates for four-hydrophone arrays that resulted in BERs of less than 1% for an SNR of 10 dB and a probability of 50%. Corresponding mode rays are shown by solid lines. The depths of mode rays at the discrete ranges of interest are shown by black dots.

than 1% for mode 1 at ranges up to 400 km with a probability of 90% are found. In this case there are a total of 3,700 arrays at 50 km and only 1 array at 300 km. It was observed that at some ranges only one hydrophone is sufficient to correctly decode the transmitted digits. This observation is not surprising at short ranges for which propagation-induced distortions are insignificant. At longer ranges good BERs could sometimes be achieved with only one hydrophone as well, but this behavior is not expected to be robust. The explanation is likely linked to the dependence of the SWDMP amplitude (and thus SNR) on propagation range. While on average (over many realizations of the perturbation field) the amplitude of a modal pulse is expected to monotonically decrease with range, this dependence might not be monotonic for a particular realization of the perturbation field resulting in clearer arrivals at longer ranges. To estimate the most likely placement of a desirable array, the mean depth and one standard deviation in depth of all hydrophones are computed at each range. The resulting two depth values (mean $\pm$ one standard deviation) for mode 1 processing are shown by short tick marks at each range in Figure 9b). The same analysis is repeated for mode 20, except that four-hydrophone arrays are considered and the desired success rate is lowered to 50%. The results are shown in Figure 9d).

To explain the observed pattern two mode rays are computed. The mode ray shown in Figure 9b) starts at the lower turning point of mode 1 (834 m), the mode ray shown in Figure 9d) starts at the average depth of the upper turning points for modes 19 and 20 at 75 Hz (231 m). The selection of the up- and down-going mode ray depends on the depth of the source relative to the turning point of the mode (an up-going ray is chosen for mode 1, and a down-going ray is chosen for mode 20). Recall that the arrays considered here are not mode resolving. The "cross-talk" between modes 19 and 20 observed with the four-hydrophone arrays is large. This is why the ray with the starting depth at the average turning depths of modes 19 and 20 agrees better with predicted array depths than the mode 20 mode ray. Overall, the agreement between array predictions based on full wave simulations and ray theory is very good for both modes 1 and 20. For mode 1 the agreement is slightly worse at short ranges suggesting that the source should be placed closer to the peak in the mode shape function, rather than along the mode ray.

It is also interesting to compare the phases of modal arrivals estimated with these short arrays to the correct phases estimated through mode filtering with the full water column array (with 5001 hydrophones). Figure 10 shows

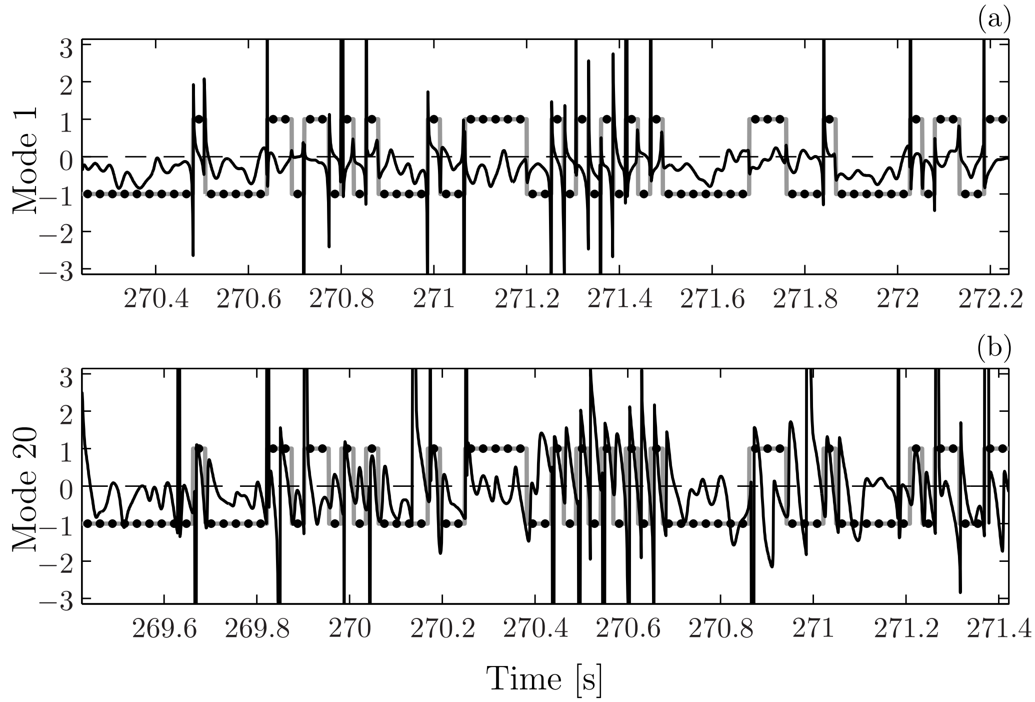

Figure 10: An example of phase errors from two-hydrophone array processing for mode 1 (top panel) and four-hydrophone array processing for mode 20 (bottom panel) at 400 km range with an SNR of 10 dB. The phase errors are shown with black solid lines. The thick gray line is the idealized transmitted square wave (with unit amplitude). The black dots show the digits recovered from the phase function. The horizontal axis is the absolute arrival time. The vertical axis on each panel shows phase errors between -π and π.

phase errors with black lines for mode 1 (top panel) and mode 20 (bottom panel) at 400 km range with an SNR of 10 dB. The time axis under each subplot shows the absolute arrival time. Thus, the mode 20 pulse arrives approximately 0.8 s earlier than the mode 1 pulse at 400 km range. Despite fairly large phase errors, phase transitions are identified correctly, and the transmitted binary sequence is recovered without errors for mode 1, and with BERs of less than 1% for mode 20 (there are no errors in the first 75 digits shown in the bottom panel of Figure 10) .

Finally, note that while the results are sensitive to the variations of modal amplitude along the propagation path due to scattering, the modal pulse spreads do not change significantly for different realizations of the IW-induced perturbation field as long as the IW model is valid (i.e. the perturbation statistics are adequately described by the Garrett-Munk spectrum). This can be seen from theoretical arguments and numerical simulations presented in earlier work. The performance of the system relying on SWDMP in terms of BERs is largely controlled by the total time spread for that modal pulse, which is described by Eq. (6) (or its variations) in [6]. The two constituents of Eq. (6), the reciprocal bandwidth contribution, and the deterministic dispersive contribution (Eqs. (7) and (8) in [6], respectively) do not depend on the properties or the statistics of the internal waves. The third term, Eq. (9) in [6], depends only on the strength of the IW-induced perturbation field through the parameter B (do not confuse it with the thermocline depth discussed in Appendix A), which does not depend on a particular realization. Thus, the total time spread variations of the modal pulse (and consequently expected BER variations) are statistically insignificant as long as the strength of the IW-induced fluctuations (and B) remains unchanged (1 nominal Garrett-Munk strength (GM) was used in all simulations). Quantitatively, time spreads may change in environments with different perturbation strength, but variations due to a particular realization are insignificant. Note, however, that the results are sensitive to the amplitude fluctuations of modal pulses along the propagation path, which are caused by scattering due to internal waves.

5. Discussion

The results presented here are expected to be useful in communications applications. Focusing on SWDMPs prior to channel equalization significantly reduces the channel delay spread thus decreasing the complexity of the required equalization scheme. The efficient use of SWDMPs with a modest number of receivers and optimal source placement could potentially be exploited for communications between moving platforms. The knowledge of the longest range that the signal propagates undistorted is also important for underwater communications.

This paper explains, using theoretical arguments and numerical simulations, how to design a long-range acoustic underwater system in the deep ocean that takes advantage of the special properties of SWDMPs. Two groups of SWDMPs are considered in typical mid-latitude ocean environments: those that correspond to low order modes (modes 1-3 at 75 Hz), and those corresponding to intermediate order modes, for which the waveguide invariant parameter is near-zero (19 and 20 at 75 Hz). It is shown that

SWDMPs corresponding to modes 1-3 may be useful in communications applications at ranges up to 500 km, which is consistent with the results of the LOAPEX data analysis [8]. For longer ranges one should take into account the mesoscale variability and variations of the background sound speed profile along the propagation path. SWDMPs corresponding to intermediate mode numbers are expected to be observable at ranges up to 400 km. There are two reasons that these modes do not perform as well as low order modes. The first reason is the scattering from nearby strongly dispersive modes in the vicinity of modes 19 and 20 (modes 15-18, for example). This scattering may cause the arrivals for modes 19 and 20 to spread. The second reason is the variation of the IW-induced fluctuation strength with depth, that is expressed through the parameter $B(m)$ and which increases approximately linearly with mode number (see Section V in [26] for the discussion of the $B(m)$ dependence). Nevertheless, both groups of weakly dispersive modes are expected to be observable at ranges of several hundreds of kilometers.

This paper shows that only a small number of hydrophones may be needed to achieve low BERs without channel equalization. With fixed receiver depths and at the ten ranges considered (between 50 km and 500 km) only 4 hydrophones are needed to achieve BERs of less than 5% using mode 1, 11 using mode 2, and 12 using mode 3 for all propagation distances provided SNR is up to 20 dB with 90% probability. For intermediate mode numbers (modes 19 and 20) around 30 hydrophones are needed. In either case the receiving array does not need to span the entire mode shape in depth. However, one needs to ensure that modal "cross-talk" caused by a short and sparse receiving array does not inhibit the demodulation algorithm from detecting the phase transitions. The guidelines for estimating optimal source depth are offered, which could be useful if one desires to operate a shallow source.

It is also shown that if the depths of the hydrophones are allowed to vary depending on the source-receiver distance, often only two hydrophones are sufficient to achieve low BERs with SWDMPs corresponding to either low order modes and three or four hydrophones could be sufficient if intermediate mode numbers are used. This would be important in a practical design if one desires to use navigated autonomous vehicles or a mooring with adjustable hydrophone depths instead of a fixed array installation. The estimates are reliable with either group of modes at ranges up to 400 km. The desirable depths of hydrophones are well predicted by ray theory with some caveats as mentioned above.

The number of hydrophones required to achieve low BERs rapidly increases as SNR decreases below approximately 10 dB. However, the LOAPEX data analysis demonstrated that desired SNRs could be achieved at ranges up to 500 km. Unfortunately, it does not seem feasible to derive simple analytical expressions for the dependencies of BERs on SNR. The resulting BERs depend on many factors besides the SNR, such as the distribution of acoustic energy in the water column and across the receiving array, the signal coherence across individual elements, the distribution of energy among modes, and the amount of modal cross-talk. These characteristics, in turn, depend on the environmental conditions, source and receiver geometries, and propagation range. Therefore, BERs in this paper are estimated numerically under various conditions.

The results presented in this paper rely on the assumption that the sound speed profile is approximated as a range-independent background profile with small range- and depth-dependent IW-induced perturbations superimposed. In environments with strong range dependence, however, similar analysis can be carried out. The results also rely on the accuracy of the 2D acoustic propagation model RAM. In environments with significant out-of-plane scattering, bottom reflections, or horizontal refraction this analysis should be revisited. Also note that while SWDMPs (or corresponding weakly divergent beams) were observed in some environments, they are not expected to be ubiquitous. A comprehensive analysis of the existence and practical usefulness of SWDMPs in various environments would be necessary.

6. Conclusions

This paper demonstrates the potential utility of SWDMPs for long-range underwater data transmission. It is shown that both groups of weakly dispersive modal pulses that commonly occur in typical mid-latitude deep ocean environments, the lowest order modes and the intermediate order modes whose waveguide invariant is near-zero, can be used at ranges up to 500 km. The guidelines for estimating the optimal source depth are provided. This paper also demonstrates that full modal resolution is unnecessary to accurately recover the information carried by SWDMPs. Therefore the requirements on the extent and the number of hydrophones in the receiving array are greatly reduced. The necessary depths of hydrophones are well predicted by acoustic ray theory.

Table A.1: Summary of the parameters used in the numerical model.

C_1 [km/s]	z_1 [km]	B [km]	ε	dc [km/s]
1.48	-0.7	0.52	0.0025	0.008
z_c [km]	z_w [km]	h [km]	ρ_w, ρ_s [kg/m^3]	$h_s [m]$
-0.35	0.1	5	1000	1000
c_s [km/s]	α_1 [dB/λ]	α_2 [dB/λ]	SL [dB]	f_{min} [Hz]
1538.67	0.05	0.35	195	37.5
f_{max} [Hz]	Δr [km]	Δz [km]	n_p	r_s [km]
112.5	0.1	0.001	4	50

Acknowledgments

The author thanks Dr. Ralph Stephen for proofreading the manuscript. The author thanks Dr. Michael Brown and Dr. Oleg Godin for valuable suggestions and recommendations. The author also thanks Dr. Timothy Duda and Dr. Ying-Tsong Lin for the PE-based numerical model used for comparison and validation of the simulated wave fields. This research did not receive any specific grant from funding agencies in the public, commercial, or not-for-profit sectors.

Appendix A.

Details of the RAM-code numerical simulations and the choice of relevant parameters are presented in this appendix. Two slightly different range-independent ocean sound-speed profiles are considered. The first profile, called C0, is the canonical "Munk" mid-latitude ocean profile. The second profile, called C1 in this paper, is the same as in [23] and is a perturbed version of C0.

All parameters of the numerical model are summarized in Table A.1. In C0, using the original "Munk" profile notation, C_1 is the sound speed at the sound channel axis, z_1 is the depth of the axis, B is the thermocline depth scale, and ε is a dimensionless constant. In the perturbed profile, $c_M(z)$ is the canonical "Munk" profile, dc is the maximum amplitude of the Gaussian perturbation, z_c is the depth of the midpoint of the Gaussian perturbation, and z_w is the width of the Gaussian perturbation. Additional environmental parameters are h, the depth of the ocean (assumed constant), ρ_w and ρ_s, densities of the water and sediment, respectively, c_s, the compressional speed of the sediment, set equal to the water sound speed at the water/sediment interface, h_s, the sediment thickness, α_1 and α_2, compressional attenuations at the top and the bottom of the sediment layer (with a linear gradient assumed in between). Acoustic parameters are source level, SL, plus f_{min} and f_{max}, the lowest and highest frequencies of interest. Computational scheme parameters are the range step Δr, the depth step Δz, the number of Padé terms n_p, and the range r_s (from the source) where the stability constraint is turned off.

While it was previously shown that bottom reflections could interfere with purely water column refracted energy at short transmission ranges [36], bottom reflections are neglected in this modeling. Bottom properties in the model are set to suppress these reflections. The IW-induced sound-speed perturbations are modeled using the procedure described by [37]. The strength of the IW-induced perturbations is one nominal Garret-Munk strength (1 GM).

The acoustic source is a phase-modulated m-sequence at 75 Hz, with 1023-digits and each digit corresponds to two cycles of the carrier frequency. The m-sequence is the same as in LOAPEX [28]. The total duration of the source signal, T_0, is 27.28 sec. The resulting spectrum is broadband with the maximum near 75 Hz, and the first nulls, f_{min} and f_{max}, near 37.5 and 112.5 Hz.

It is important to note a few subtleties in the construction of the analyzed wave fields, an example of which is shown in Figure 3. To fit the entire reception into the model time window at long ranges, the window must be longer than T_0. The window length is given by the inverse of the frequency spacing. The selection of 4,092 computed frequencies covering $f_{\max} - f_{\min}$ (75 Hz), gives a sufficient window length of $2T_0$. Therefore, the actual source function used in simulations consisted of the 27.28 s signal and an equally long period of silence. It is well known that this type of source function is not compatible with optimal two-state correlation processing of m-sequences to estimate impulse response (i.e. arrivals shown in Figures 3b) and 3d). To analyze a pulse-compressed signal with a source function duration of $2T_0$, the source signal should consist of exactly two periods of the m-sequence. This is unnecessary here, however, because the objective is to analyze modal arrivals *before* pulse compression, with no attention paid to special properties of the m-sequences. The only consequence of the chosen T_0-length source function is the presence of energy leakage across time (temporal sidelobes) in both

Figures 3b) and 3d). These pulse-compressed arrivals, however, are shown for illustration purposes only and are not further analyzed. Note that the same 4,092 frequencies were used for the computation of normal modes and for the mode filtering. Modes were computed using the KRAKEN normal mode code [38].

Appendix B.

The details describing the selected array configurations are presented in this appendix. Two sets of receiving arrays are considered in this paper: one in C0 and the other in C1 environments. The main difference between the two sets is that they span different depth apertures. All considered hydrophones are placed between $h_1 = 120$ m and $h_2 = 1660$ m depths in C0 and between $h_1 = 0$ m and $h_2 = 3400$ m depths in C1. In both environments the minimum hydrophone separation, the separation increment, and the the depth-step for the shallowest hydrophone are the same and equal to $\Delta h = 5$ m. The number of hydrophones in all tested arrays varies between 2 and the maximum number that fits into the depth aperture with the minimum separation, i.e. (1660-120)/5+1=309 in C0 and (3400-0)/5+1=681 in C1. The total number of 2-element arrays is

$$\frac{h_2 - h_1}{\Delta h} + \left(\frac{h_2 - h_1}{\Delta h} - 1\right) + \left(\frac{h_2 - h_1}{\Delta h} - 2\right) + ... + \left(\frac{h_2 - h_1}{\Delta h} - \left(\frac{h_2 - h_1}{\Delta h} - 1\right)\right) = \frac{h_2 - h_1}{2\Delta h} \times \left(\frac{h_2 - h_1}{\Delta h} + 1\right), \tag{B1}$$

which is 47,586 in C0 and 231,540 in C1. The total number of 3-element arrays is

$$\left(\frac{h_2 - h_1}{\Delta h} - 1\right) + \left(\frac{h_2 - h_1}{\Delta h} - 3\right) + ... + \left(\frac{h_2 - h_1}{\Delta h} - \left(\frac{h_2 - h_1}{\Delta h} - 1\right)\right) = \left(\frac{h_2 - h_1}{2\Delta h}\right)^2, \tag{B2}$$

which is 23,716 in C0 and 115,600 in C1. In general, the total number of k-element arrays is

$$\sum_j \left(\frac{h_2 - h_1}{\Delta h} - (j \times (k-1) - 1)\right), \tag{B3}$$

where the sum is taken over all such integer j's that result in all terms under the summation being positive. It is easy to confirm numerically that the total number of arrays considered is 257,292 in C0 and 1,432,727 in C1 environments.

References

[1] A. L. Virovlyansky, Ray theory of long-range sound propagation in the ocean, Institute of Applied Physics, Nizhny Novgorod, Russia (in Russian), 2006.

[2] A. L. Virovlyansky, A. Y. Kazarova, L. Y. Lyubavin, Ray-based description of normal modes in a deep ocean acoustic waveguide, Journal of the Acoustical Society of America 125 (2009) 1362–1373.

[3] K. E. Wage, Broadband modal coherence and beamforming at megameter ranges, Ph.D. thesis, Massachusetts Institute of Technology (2000).

[4] K. E. Wage, A. B. Baggeroer, J. C. Preisig, Modal analysis of broadband acoustic receptions at 3515-km range in the North Pacific using short-time Fourier techniques, Journal of the Acoustical Society of America 113 (2003) 801–817.

[5] K. E. Wage, M. A. Dzieciuch, P. F. Worcester, B. M. Howe, J. A. Mercer, Mode coherence at megameter ranges in the North Pacific Ocean, Journal of the Acoustical Society of America 117 (2005) 1565–1581.

[6] I. A. Udovydchenkov, M. G. Brown, T. F. Duda, J. A. Mercer, R. K. Andrew, P. F. Worcester, M. A. Dzieciuch, B. M. Howe, J. A. Colosi, Modal analysis of the range evolution of broadband wavefields in the North Pacific Ocean: Low mode numbers, Journal of the Acoustical Society of America 131 (2012) 4409–4427.

[7] M. G. Brown, I. A. Udovydchenkov, Underwater communication using weakly dispersive modal pulses, Acoustical Physics 59 (2013) 533–538.

[8] I. A. Udovydchenkov, M. G. Brown, T. F. Duda, P. F. Worcester, M. A. Dzieciuch, J. A. Mercer, R. K. Andrew, B. M. Howe, J. A. Colosi, Weakly dispersive modal pulse propagation in the North Pacific ocean, Journal of the Acoustical Society of America 134 (2013) 3386–3394.

[9] M. Stojanovic, J. A. Catipovic, J. G. Proakis, Reduced-complexity spatial and temporal processing of underwater acoustic communication signals, Journal of the Acoustical Society of America 98 (1995) 961–972.

[10] H. C. Song, B. M. Howe, M. G. Brown, R. K. Andrew, Diversity-based acoustic communication with a glider in deep water, Journal of the Acoustical Society of America 135 (2014) 1023–1026.

[11] A. Song, M. Badiey, H. C. Song, W. S. Hodgkiss, M. B. Porter, the KauaiEx Group, Impact of ocean variability on coherent underwater acoustic communications during the Kauai experiment (KauaiEx), Journal of the Acoustical Society of America 123 (2008) 856–865.

[12] L. Freitag, M. Stojanovic, Basin-scale acoustic communication: a feasibility study using tomography m-sqeuences, OCEANS, MTS/IEEE Conference and Exhibition 4 (2001) 2256 – 2261.

[13] S. D. Chuprov, Selection of modes and rays in underwater sound channels, in: Acoustics of the Ocean Medium, Nauka, Moscow (in Russian), 1989, pp. 56–64.

[14] Y. V. Petukhov, A sound beam with minimal wavefront divergence in a stratified ocean waveguide, Acoustical Physics 40 (1994) 97–105.

[15] Y. V. Petukhov, Slowly-diverging acoustics beams in smoothly inhomogeneous ocean wavefguides, Acoustical Physics 43 (1997) 196–201.

[16] L. M. Brekhovskikh, V. V. Goncharov, S. A. Dremuchev, V. M. Kurtepov, V. G. Selivanov, Y. A. Chepurin, Long range sound propagation experiment in the Canarian Abyssal Plain, the Atlantic, Acoustical Physics 36 (1990) 824–831.

[17] L. M. Brekhovskikh, V. V. Goncharov, V. M. Kurtepov, Weakly divergent bundles of rays and their possible use in inverse methods of ocean acoustics, in: Full field inversion methods in ocean and seismo-acoustics, Kluwer Academic Publishers, Dordrecht, Netherlands, 1995, pp. 39–44.

[18] L. M. Brekhovskikh, V. V. Goncharov, V. M. Kurtepov, Weakly divergent bundles of sound rays in the Arctic, Atmospheric and Oceanic Physics 31 (1995) 441–446.

[19] V. V. Goncharov, V. M. Kurtepov, Formation and propagation of weakly diverging bundles of rays in a horizontally inhomogeneous ocean, Acoustical Physics 40 (1994) 685–692.

[20] M. G. Brown, F. J. Beron-Vera, I. Rypina, I. A. Udovydchenkov, Rays, modes, wavefield structure, and wavefield stability, Journal of the Acoustical Society of America 117 (2005) 1607–1610.

[21] F. J. Beron-Vera, M. G. Brown, Underwater acoustic beam dynamics, Journal of the Acoustical Society of America 126 (2009) 80–91.

[22] W. H. Munk, Sound channel in an exponentially stratified ocean with application to SOFAR, Journal of the Acoustical Society of America 55 (1974) 220–226.

[23] I. I. Rypina, I. A. Udovydchenkov, M. G. Brown, A transformation of the environment eliminates parabolic equation phase errors, Journal of the Acoustical Society of America 120 (2006) 1295–1304.

[24] R. A. Stephen, P. F. Worcester, I. A. Udovydchenkov, E. Aaron, S. T. Bolmer, S. Carey, S. P. McPeak, S. A. Swift, M. A. Dzieciuch, Cruise report: Ocean Bottom Seismometer Augmentation in the North Pacific (OBSANP), Tech. Rep. WHOI-2014-03, Woods Hole Oceanographic Institution, Woods Hole, MA (2014).

[25] S. D. Chuprov, Interference structure of a sound field in a layered ocean, Ocean Acoustics, Current State, (1982) 71–91.

[26] I. A. Udovydchenkov, M. G. Brown, Modal group time spreads in weakly range-dependent deep ocean environments, Journal of the Acoustical Society of America 123 (2008) 41–50.

[27] D. Makarov, S. Prants, A. L. Virovlyansky, G. Zaslavsky, Ray and wave chaos in ocean acoustics, World Scientific, Hackensack, New Jersey, USA, 2010, p. 389 pages.

[28] J. A. Mercer, R. K. Andrew, B. M. Howe, J. A. Colosi, Cruise report: Long-range ocean acoustic propagation experiment (LOAPEX), Tech. Rep. APL-UW TR0501, Applied Physics Laboratory, University of Washington, Seattle, WA (2005).

[29] J. A. Mercer, J. A. Colosi, B. M. Howe, M. A. Dzieciuch, R. Stephen, P. F. Worcester, LOAPEX: The Long-Range Ocean Acoustic Propagation EXperiment, IEEE Journal of Oceanic Engineering 34 (2009) 1–11.

[30] M. D. Collins, E. K. Westwood, A higher-order energy-conserving parabolic equation for range-dependent ocean depth, sound speed and density, Journal of the Acoustical Society of America 89 (1991) 1068–1075.

[31] M. Collins, A split-step Padé solution for the parabolic equation method, Journal of the Acoustical Society of America 93 (1993) 1736–1742.

[32] Y.-T. Lin, T. F. Duda, A. E. Newhall, Three-dimensional sound propagation models using the parabolic-equation approximation and the split-step Fourier method, Journal of Computational Acoustics 21 (2013) 1250018–1–1250018–24.

[33] T. W. Parks, C. S. Burrus, Digital Filter Design, John Wiley and Sons, Inc., New York, New York, 1987, Ch. 7, pp. 161–171, 213–218.

[34] A. Oppenheim, R. W. Schafer, J. R. Buck, Discrete-Time Signal Processing, Prentice-Hall, Inc., Upper Saddle River, New Jersey, 1999, Ch. 5.6, pp. pp. 280–291.

[35] J. R. Buck, J. C. Preisig, K. E. Wage, A unified framework for mode filtering and the maximum a posteriori mode filter, Journal of the Acoustical Society of America 103 (1998) 1813–1824.

[36] I. A. Udovydchenkov, R. A. Stephen, T. F. Duda, S. T. Bolmer, P. F. Worcester, M. A. Dzieciuch, J. A. Mercer, R. K. Andrew, B. M. Howe, Bottom interacting sound at 50 km range in a deep ocean environment, Journal of the Acoustical Society of America 132 (2012) 2224–2231.

[37] J. A. Colosi, M. G. Brown, Efficient numerical simulation of stochastic internal-wave-induced sound speed perturbation fields, Journal of the Acoustical Society of America 103 (1998) 2232–2235.

[38] M. B. Porter, The KRAKEN normal mode program. rep. sm-245, Tech. rep., SACLANT Undersea Research Centre, La Spezia, Italy (1991).

List of Figures